Resolution of 2D Wenner resistivity imaging as assessed by numerical modelling

Dahlin, Torleif; Loke, Meng Heng

Published in:
Journal of Applied Geophysics

DOI:
10.1016/S0926-9851(97)00030-X

1998

ELSEVIER

Journal of Applied Geophysics 38 (1998) 237–249

JOURNAL OF APPLIED GEOPHYSICS

Resolution of 2D Wenner resistivity imaging as assessed by numerical modelling

T. Dahlin [a,*], M.H. Loke [b,1]

[a] *Dep. of Geotechnology, Lund University, Box 118, 221 00 Lund, Sweden*
[b] *School of Physics, University Sains Malaysia, 11800 Penang, Malaysia*

Received 16 April 1997; accepted 23 September 1997

Abstract

Modelling of 2D resistivity imaging was done in order to understand the principle resolution of the technique in different geological situations, and for assessing the behaviour of the interpretation methods under controlled circumstances. The Wenner array was used throughout. The results show that the 1D approximation only provides reasonable results in environments with very gradual lateral resistivity changes, otherwise the result may be strongly misleading. Inversion using the 2D quasi-Newton technique results in adequate resolution of the structures in moderately complex environments, but the Gauss–Newton method holds a significant advantage in some complicated cases. The data density can also be of crucial importance for the resolution capability, notably of narrow structures. © 1998 Elsevier Science B.V.

Keywords: DC resistivity; Wenner array; numerical modelling; inversion; imaging

1. Introduction

DC resistivity data acquisition using computer controlled multi-electrode arrays is becoming increasingly popular, as it allows efficient and complex data acquisition strategies that are inconceivable with manual methods. The trend is expected to continue because there is an increasing demand for detailed knowledge about sub-surface features in environmental, hydrogeological and engineering applications. A variety of commercially available acquisition systems are available on the market, and the capacity of the instruments will increase in the future. The continued development of efficient techniques for data inversion and imaging facilitate interpretation and presentation of the data.

However, the ability of the DC resistivity method to resolve complex structures is not fully known, and with the continued development of data acquisition and inversion techniques the resolution capability is evolving. Since it is impossible to gain a full control of the subsurface structures in natural geological environments, modelling is necessary for testing interpretation methods under controlled circumstances. Therefore, numerical modelling of 2D resistivity imaging was done in order to gain a better understanding of the resolution in differ-

* Corresponding author. E-mail: torleif.dahlin@tg.lth.se.
[1] E-mail: mhloke@usm.my.

PII S0926-9851(97)00030-X

ent representative geological situations, and for assessing the behaviour of some interpretation methods.

Throughout, the modelling emulated 2D profiling with the Wenner array, which is also referred to as CVES (continuous vertical electrical sounding). This measurement strategy is commonly used for field surveying with some of the commercially available data acquisition systems.

2. Method

The finite difference (FD) method was employed for the forward modelling, where the modelling routine accounts for 3D sources (current electrodes) in a 2D material model, sometimes referred to as 2.5D modelling. This means that the resistivity can vary arbitrarily along the line of surveying (x-direction) and with depth (z-direction), but the models have an infinite perpendicular extension (y-direction). The program used (RES2DMOD) is a modification of the classic code described by Dey and Morrison (1979) and (Loke and Barker, 1996).

The modelled geometrical resolution simulates the one obtained with a commercially available system, the ABEM Lund Imaging System. In all cases a layout of 101 electrodes was modelled, with an electrode separation of one length unit. This is equal to doing one roll-along with the data acquisition system in question, plus measuring with the instrument at the outer cable intersections of the first and last cable layouts. Throughout, the Wenner array and the standard system configuration of the Lund Imaging System was modelled. However, to assess the combined influence of noise and data density, variations in data point density were modelled in some cases. In the case of field data acquisition, this data point density would depend only on the protocol files chosen, if standard electrode cables were used.

Calculation errors were assessed by comparing the model response of some models where analytical responses are available:

(1) Vertical outcropping contact (Carpenter, 1955);

(2) Horizontal two-layer with ascending resistivity (Telford et al., 1990);

(3) Horizontal two-layer with descending resistivity (Telford et al., 1990).

The calculation errors are highly dependent on the discretisation, and the figures presented here relate to an example of an upper layer thickness of 2.2 units for the two-layer cases, using the layer depth distribution in Table 1. The calculation errors were relatively low for the first 2 cases (Table 2), with maximum errors of less than 3% within a resistivity contrast range of 10^1 to 10^3. For the descending two-layer case, however, maximum calculation errors were 2.3% for a resistivity contrast of 10^1, with approximately doubled calculation errors for each order of magnitude in contrast, giving

Table 1
Layer depths of forward finite difference models, with a lateral discretisation of 0.5 units (i.e. 2 finite difference cells between each electrode)

Layer #	Depth/[-]
1	0.3
2	0.6
3	0.9
4	1.2
5	1.5
6	2.2
7	3.5
8	4.92
9	6.5
10	8.22
11	10.12
12	12.22
13	14.52
14	17.06
15	19.84
16	23.46
17	28.18
18	34.3
19	42.26
20	52.6
21	66.06
22	83.56

Table 2
Range of calculation errors for forward modelling, in terms of lowest and highest deviation from analytical model response

Model	Contrast		
	10 to 100	10 to 1000	10 to 10,000
Vertical contact	−1.2/1.4	−1.2/1.6	−1.3/1.7
Ascending 2 layer	−1.4/−0.5	−2.4/−1.2	−2.8/−1.1
Descending 2 layer	−2.3/1.8	−4.3/1.8	−7.6/3.7

7.6% error for a contrast of 10^3. The calculation error of the two-layer models increase with decreasing thickness of the top layer, and a thickness of 0.6 units of the top layer (comprising only the top 2 rows of model cells) results in 5.6% maximum error for the 10^1 contrast ascending model.

Gauss distributed random noise was added to the calculated responses for some of the models, to test the sensitivity of the interpretation routines. In general, noise with 5% standard deviation was added. Experience with Wenner surveying in Sweden, including CVES as well as Offset Wenner sounding, shows that pure measurement errors can normally be kept less than 1%, if good electrode contact is provided (Dahlin, 1993). The measurement errors can be assessed by reversing current and potential electrode positions and applying the reciprocity theorem (e.g. Parasnis, 1986). These measurement errors are supported by experience from Zimbabwe (Barker et al., 1992). On sites with higher electrode contact resistances, however, it may be reasonable to expect higher measurement uncertainties. In addition, the effect of small-scale geological inhomogeneities, of the size that cannot be accounted for in the models, can also be regarded as noise.

In the 1D inversion or imaging the data are regarded as a series of closely spaced VES, which are evaluated one after the other. This was carried out using least-squares inversion similar to the Gauss–Newton method described below (Christensen and Auken, 1992), as well as with the method presented by Zhody (1989). The resulting resistivity depth models are then stacked together to obtain quasi-2D sections. The major advantage of the Zohdy technique is that it is very fast. It can thus be used on small portable computers used for data acquisition in the field, which are often not equipped with powerful processors. The 1D inversion code tried here was much slower than the 1D Zohdy imaging as well as the 2D quasi-Newton inversion, where the number of iterations used for each model was up to 20 but normally the process was aborted earlier. The two different types of 1D results are essentially the same, and due to space limitations only the 1D inversion results are presented in the sections below.

The 2D inversion is based on the generation of a finite difference (FD) model of the subsurface, where the model resistivities of the FD grid are automatically adjusted through an iterative process so that the model response converges towards the measured data (Loke and Barker, 1996). Both the quasi-Newton and Gauss–Newton method are smoothness-constrained least-squares inversion methods, where by default the vertical and horizontal smoothness constrains are the same (DeGroot-Hedlin and Constable, 1990). The smoothness constrain increases with 10% per layer, which along with increasing layer thickness reduces the resolution with depth.

The quasi-Newton inversion is based on an analytical calculation of the sensitivity matrix (Jacobian matrix) for a homogeneous halfspace for the first step of iteration. The sensitivity matrix is used for updating the model resistivities at each step of iteration, and it will change with the change of the resistivity distribution within the model due to the non-linear character of the problem. The quasi-Newton method is used to reduce the numerical calculation, by means of a fast approximate update of the sensitivity matrix, so that only the forward response of the new resistivity model requires re-calculating with the FD method for each step of iteration. This approach can be expected to work well for small resistivity contrasts but not necessarily for larger contrasts.

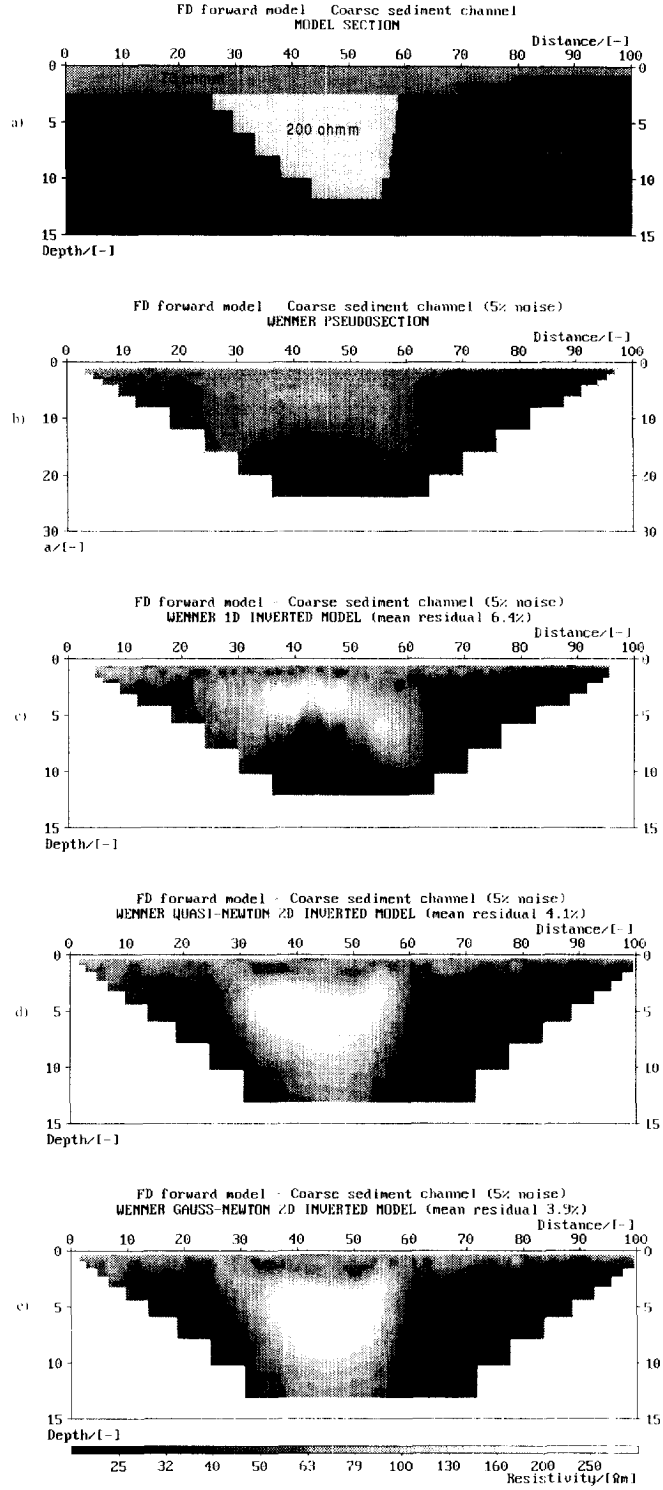

Fig. 1. Buried channel model: (a) model section; (b) pseudosection with 5% noise; (c) 1D inversion section; (d) quasi-Newton inversion section; (e) Gauss–Newton inversion section. The same grey scale is used throughout.

The 2D Gauss–Newton inversion is similar to the quasi-Newton inversion just described, but the sensitivity matrix is re-calculated using the FD method at each step of iteration. This makes the process much more time consuming than the quasi-Newton method, but the result can be expected to be better for large resistivity contrasts and complex resistivity distributions.

For the 2D inversion the same parameters were used for both types of inversion, default smoothness constraints and a vertical-to-horizontal filter ratio set to unity. Six iterations were used throughout, since after 5–6 iterations the model residuals normally do not change much. The least-squares formulation used applies a smoothness constraint on the model perturbation vector only, and not directly on the model resistivity values. In most cases, it will produce a model with a reasonably smooth variation in the resistivity values. In some cases, particularly for very noisy data sets, better results might be obtained by applying a smoothness constraint on the model resistivity values as well. Results obtained with this option are presented for the last model data set below.

3. Models of relevant geological structures

The model responses of some ideal resistivity distributions of geological relevance were calculated using the 2.5D finite difference program. The calculated model responses were used as input for the one-dimensional and two-dimensional interpretation routines.

Some illustrative examples are given in the section below. Throughout this section the following graphical presentations are made for each model:

(a) Model section;

(b) Pseudosection of model response with noise added;

(c) 1D inversion (1D Zohdy imaging looks similar but is left out for space reasons);

(d) 2D quasi-Newton inversion;

(e) 2D Gauss–Newton inversion.

3.1. Buried channel of coarse grained sediments

The model as shown in Fig. 1a consists of a 2.5-units-thick upper layer of 70 Ωm resistivity that decreases in thickness towards the right end of the model. This layer rests on a bottom layer of 30 Ωm and has embedded a triangular zone of 200 Ωm reaching to a maximum depth of 12 units. Geologically this could be a simplified model of an old river channel in a clayey environment, which has been covered by silty sediments.

The pseudosection (Fig. 1b) reveals a high resistive feature with marked lateral effects that corresponds to the 'sand channel'.

The 1D section (Fig. 1c) strongly amplifies the lateral effects and produces an image that does not at all reflect the extension of the highly resistive body, so that not even the correct centre of the structure is localised. This figure clearly shows that the depth estimations that can be made using 1D (VES) techniques over this kind of structure can be strongly misleading.

In contrast, both 2D inversion sections reflect the principal structure quite well (Fig. 1d and e). The noise produces an undulating appearance of the thickness of the top layer. It may also be noted that the top layer appears to be slightly thicker over the low resistive areas than over the high resistive channel in the inverted sections.

3.2. Waste ponds

This example was inspired by a field survey over a waste pond site in southern Sweden, where a number of pits were excavated in limestone quarry waste fill material. The pits were used for disposing various waste sludge, containing heavy metals, organic compounds etc., which were characterised by distinct low resistive anomalies (Bernstone and Dahlin, 1996). The limestone fill material was modelled to have a resistivity of 100 Ωm, while the sludge ponds were given the resistivity 10 Ωm (Fig. 2a). The sludge pond features were modelled to have different thicknesses, and some were buried at various depths.

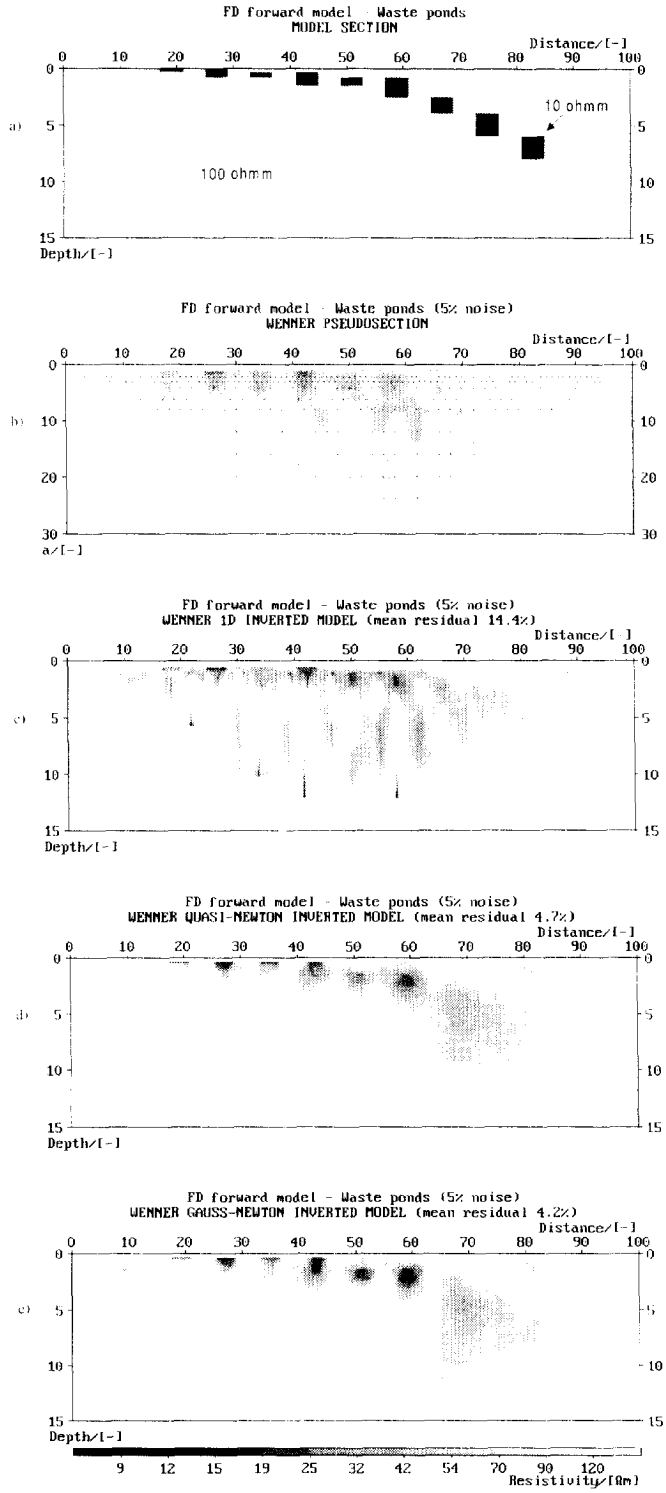

Fig. 2. Waste pond model: (a) model section; (b) pseudosection with 5% noise; (c) 1D inversion section; (d) quasi-Newton inversion section; (e) Gauss–Newton inversion section. The same grey scale is used throughout.

The pseudosection (Fig. 2b) displays a number of near surface low resistive anomalies, which correspond to the position of the low resistive bodies for those buried near the surface. The effect of those buried at some depth in the right part of the model create a blurred low resistive zone. Lateral effects create a very marked pattern for the longer electrode spacings.

The lateral effects are again strongly amplified by the 1D inversion (Fig. 2c), and the only benefit is some indication on the depth to the top of the low resistive bodies although the form of the anomalous bodies are severely disturbed. Below the level of the anomalous bodies a very marked pattern of lateral effects stand out.

Both the quasi-Newton (Fig. 2d) and Gauss–Newton (Fig. 2e) 2D inversion were successful in depicting the anomalous bodies up to the one at around 60 units on the distance scale, but for the last three bodies the inversion produces a large combined and smeared-out anomaly. There is an appearance of downward continuation for some of the anomalous bodies that may give a false impression of downward movement of contaminants. This appearance is partially related to effects of the random noise. A few weak false anomalies are seen near the right and left ends of the inverted sections, that are also noise effects, which do not appear in the corresponding inversion from noise free data. There is a slight difference in the definition of the anomalies in favour of the Gauss–Newton method.

3.3. Faulted blocks with overburden

The model in Fig. 3a is intended to model a rock sequence of faulted blocks of different widths, with alternating lower (100 Ωm) and higher (300 Ωm) resistivities than the top layer (200 Ωm). Geologically this could be faulted blocks of sedimentary rock under a layer of till or coarse-grained sediments. In the left half of the model each block is 10 units wide, whereas in the right half the blocks are 20 units wide.

The pseudosection (Fig. 3b) has a complex appearance, and it would be difficult to imagine what structure it reflects without knowing it. In the right part of the pseudosection there is a reasonable agreement between apparent resistivities and the modelled structure, whereas in the left part lateral effects create a complicated image.

The 1D inversion (Fig. 3c) makes things worse by amplifying lateral effects, and this quasi-2D image essentially only serves to create confusion. It stands clear that the 1D approximation is insufficient in this case.

The benefits of a 2D approach are illustrated by the quasi-Newton inversion (Fig. 3d), which resolves the model structure quite well. The resolution is best at shallow depths, as can be expected, and the structure blurs out to some extent at depth. Finally, the Gauss–Newton section (Fig. 3e) displays a slightly better resolution of the model.

3.4. Narrow low resistive dyke with overburden

The dyke model presented in Fig. 4a consists of a 5-units-wide low resistive (50 Ωm) dyke in an environment of high resistivities (1000 Ωm). The dyke structure is covered by a 2.5-units-thick layer of 200 Ωm. Geologically this situation could be a fractured/weathered zone in crystalline rock, under a cover of sediments or till.

The pseudosection (Fig. 4b) displays an anomaly over the location of the dyke, but it is far from evident that it reflects a vertical dyke.

The 1D inversion (Fig. 4c) amplifies the lateral effects from the pseudosection, and it does not in any way suggest the presence of a dyke structure.

Neither does the quasi-Newton inversion (Fig. 4d) manage to produce an image that comes near a vertical dyke, it rather suggests a shallow feature or a variation in depth of the upper layer.

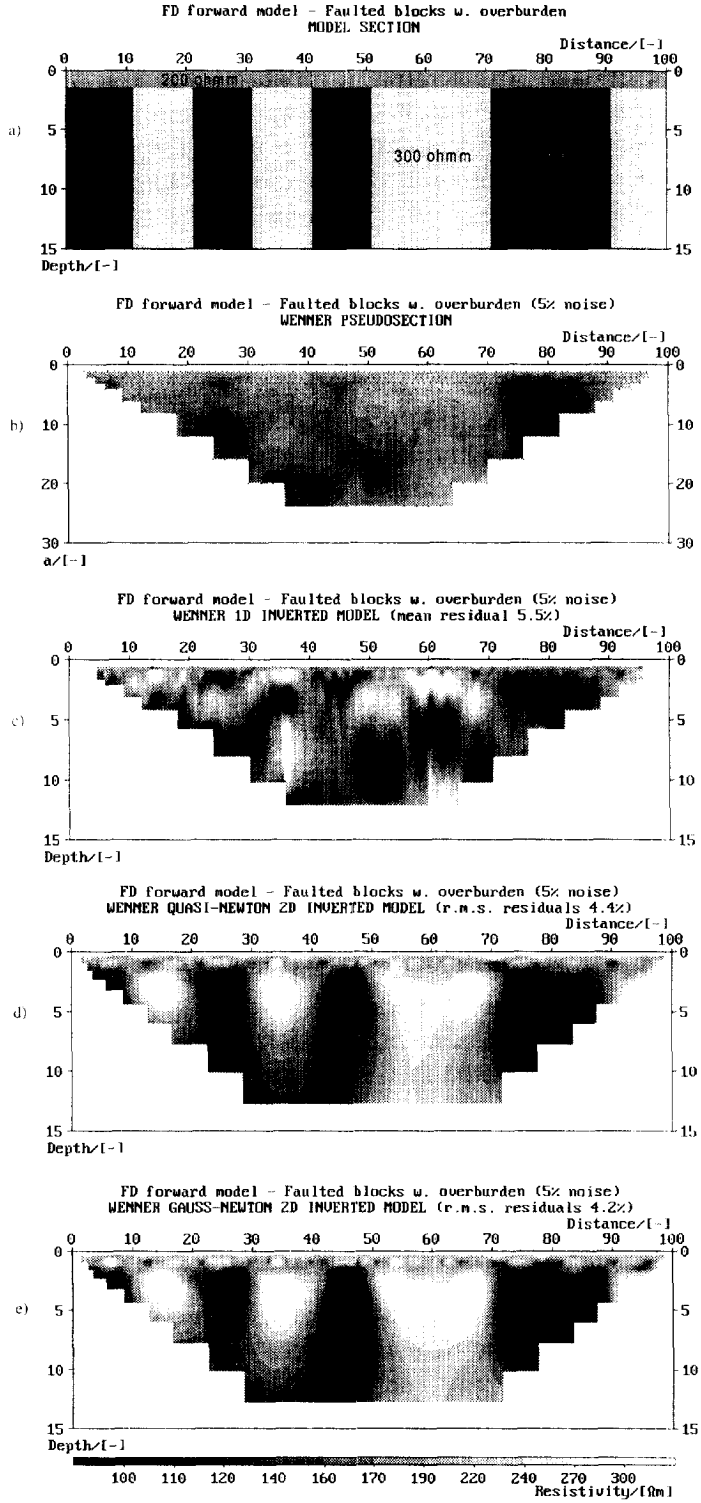

Fig. 3. Faulted blocks model: (a) model section; (b) pseudosection with 5% noise; (c) 1D inversion section; (d) quasi-Newton inversion section; (e) Gauss–Newton inversion section. The same grey scale is used throughout.

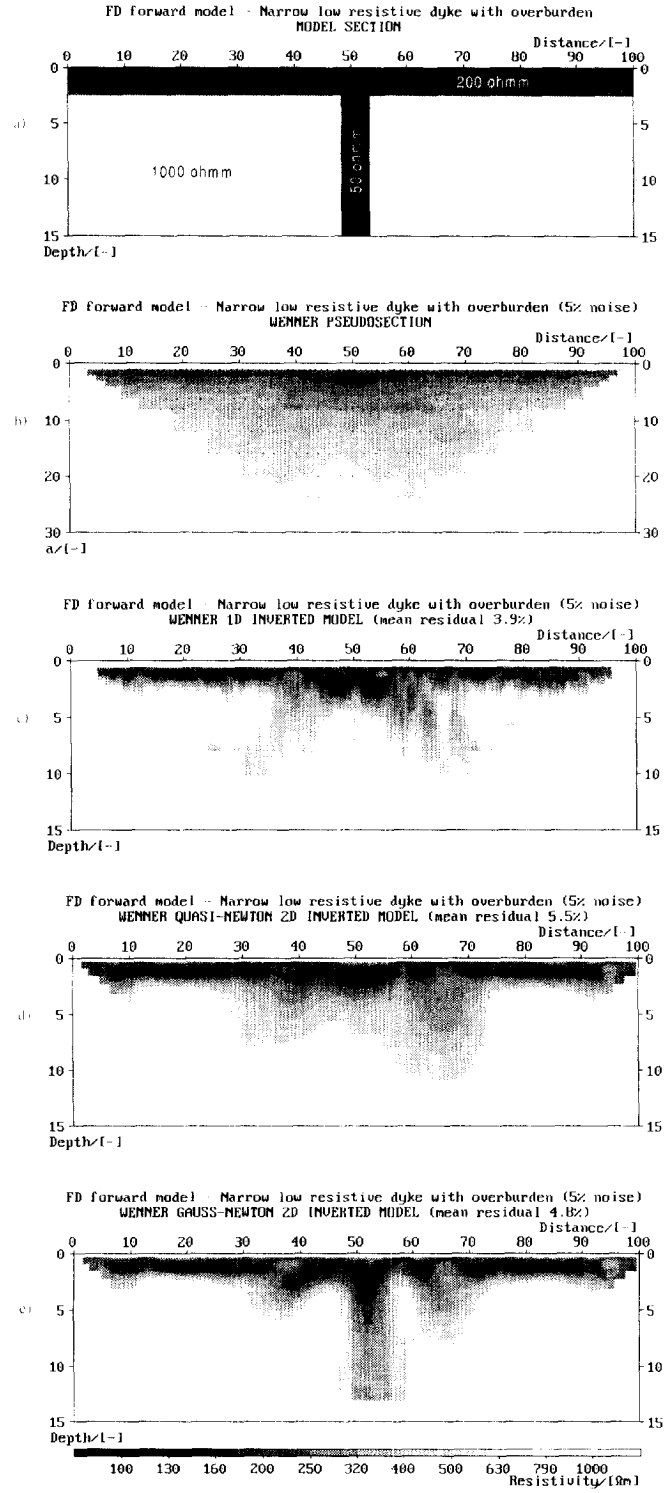

Fig. 4. Narrow low resistive dyke model: (a) model section; (b) pseudosection with 5% noise; (c) 1D inversion section; (d) quasi-Newton inversion section; (e) Gauss–Newton inversion section. The same grey scale is used throughout.

Only the Gauss–Newton inversion (Fig. 4e) arrives at a model section that reflects the dyke structure, although the dyke is not very well defined and the are apparent increased depths of the top layer on both sides of the dyke as an artifact. The structure is significantly better resolved when using smoothing of the model resistivities with the Gauss–Newton method, as is discussed below (Fig. 6b).

This example clearly demonstrates how difficult it is to resolve narrow vertical structures with Wenner CVES, but improvements in inversion techniques in recent years has made it possible to resolve features that previously could not be easily detected.

4. Data density, noise and resolution

It is sometimes argued that there is no point in using a dense measurement pattern for long electrode separations, since the resolution of the method decreases logarithmically with depth. Thus, a measurement pattern that becomes coarser with increasing electrode separation could be employed to save time in the field, as the actual measurements with a single channel instrument are quite time consuming.

On the other hand, the noise levels generally increase with increasing electrode separation in real life, as the signal-to-noise ratio decreases due to longer cable layouts and smaller measured potentials. With a coarse data pattern is it more difficult to have control over the data quality, and a few data points with high noise levels could affect the ability to resolve the structures seriously.

Model responses with three different data densities were used to assess the effect on the resolving capacity of 2D inversion, as illustrated in Fig. 5. The data densities were also modelled after the ABEM Lund Imaging System. The first (Fig. 5a) is identical to the one achieved with a prototype of the system built at Lund University, where the resolution of the Wenner array used for this measurement protocol is limited by the hardware design. The second (Fig. 5b) is the resolution achieved with the most commonly used protocol files for Wenner CVES with the commercial system available today, while the last (Fig. 5c) simulates an increased data density that can be attained with the same hardware but a modified protocol file. In all cases presented here 5% Gaussian noise was added to the model response data.

A number of different resistivity distributions were modelled, which were inverted with different set-up parameters. For relatively simple model sections the difference in inversion output is not dramatic, but for more complicated structures the resolution capacity can vary significantly. As an example, the result for the narrow low resistive dyke presented previously is shown in Fig. 6. The presented sections were inverted using the Gauss–Newton technique using the same parameters as before but also smoothing of the model resistivities.

It is clear that the data density attained with the prototype version of the system is insufficient to resolve the dyke structure with the modelled noise level (Fig. 6a), the inverted section rather reflects an increased depth of the upper layer. The normal data density results in a section (Fig. 6b) that depicts the dyke structure as well as the upper layer. It is noteworthy that the definition of the structure is significantly better with the smoothing of the model resistivities (Fig. 6b) than without (Fig. 4e), with all other factors kept identical. However, this is the case for this particular model but does not seem to be so in general. A decreasing resolution with depth is clearly seen, and there are still apparent increased depths of the upper layer appearing on both sides of the dyke. Increasing the data density results in an even better resolution of the structure (Fig. 6c), where both the dyke and the upper layer are more well defined.

From the example shown it is clear that a sufficiently high data density is of fundamental importance for the resolution of complicated structures. Regarding noise, it can be expected that the more data the better control over the

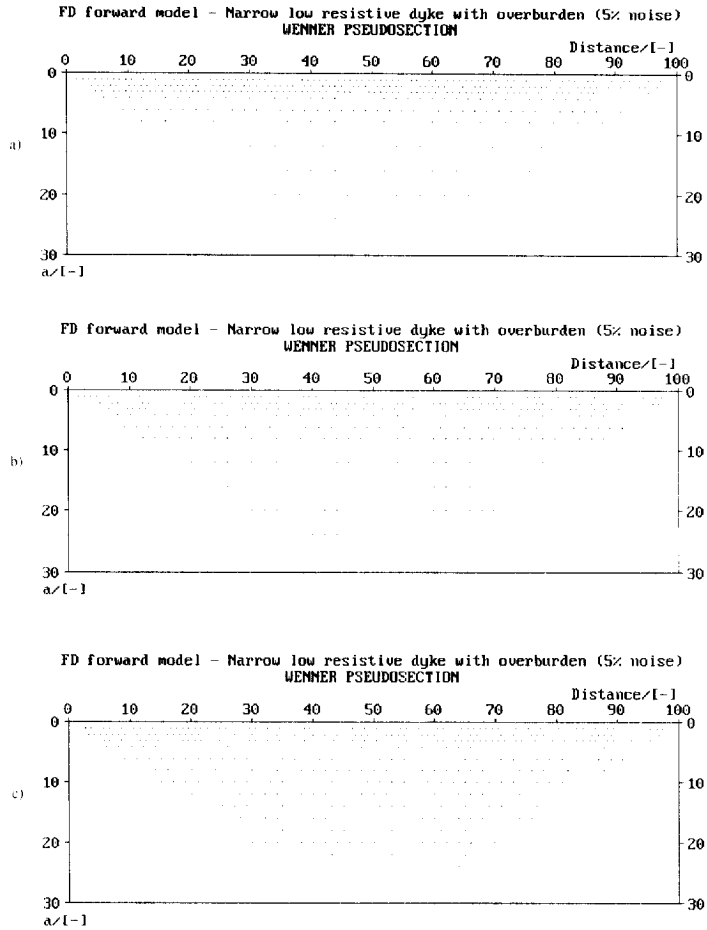

Fig. 5. The three different modelled data densities plotted as pseudosection points: (a) prototype data distribution; (b) standard data distribution; (c) enhanced data distribution.

noise can be, provided the average noise level remains the same. In practice, however, the data point density will have to be a trade-off against total measuring time, but with new, faster instruments appearing on the market the measuring time will be a less critical factor.

5. Conclusions

Pseudosection plotting is an important tool for data quality estimation, provided the plotting is carried out with no smoothing, as poor quality data points will immediately stand out. Pseudosections can also be useful for a preliminary qualitative interpretation, but in complex environments it may be difficult to perceive the structure behind the section.

One-dimensional data acquisition, imaging and inversion (VES) techniques can be strongly misleading when used over 2D structures. It is easy to realise that a limited number of traditional resistivity soundings carried out over any of the situations modelled here would not provide adequate results. However, if carried out as pairs of orthogonal soundings, the difference in results between the two layout directions would warn against putting any confidence in the results. If used with caution, 1D Zohdy imaging

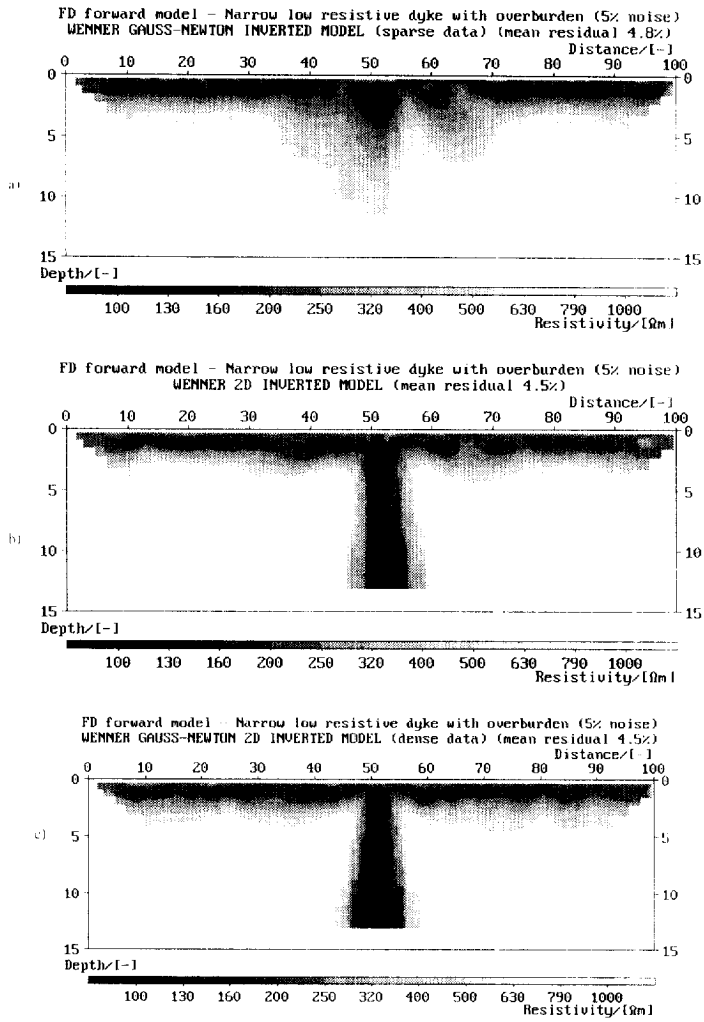

Fig. 6. Narrow low resistive dyke model (same as in Fig. 4), inverted sections resulting from the three different data densities shown in Fig. 5: (a) prototype data distribution; (b) standard data distribution; (c) enhanced data distribution. In this case smoothing of model resistivities was used.

can be suitable for a preliminary data evaluation in the field, due to the speed of the calculations, but any significant lateral change will be strongly amplified and thus misleading. However, with faster field computers the 2D deconvolution technique suggested by Møller et al. (1996) will probably be more attractive in the near future.

The 1D inversion tested here took about 15 min on a Pentium 90 based computer for inverting the soundings corresponding to one of the sections, but this cannot be compared to the figures for the 2D inversion below as the number of iterations were larger and the code not optimised for speed of operation in this application. The results obtained with the 1D approximation does not motivate further efforts on this line, whereas 1D analysis of extracted data sets from areas where the lateral variation is small can shed additional light on the layer parameters.

The quasi-Newton technique gives good results in areas with moderate resistivity contrasts and complexity. A major advantage is the fast

processing, 6 iterations with a data sets the size presented here takes about 3 min on a computer equipped with a Pentium 90 processor.

The Gauss–Newton technique is superior in some cases, notably for narrow vertical structures and large resistivity contrasts. The price for the improved performance is more intensive processing, a typical inversion of one of the above data sets took around 30 min under the same conditions as for the quasi-Newton method.

It is also clear that the data density is an important factor in resolving certain structures. Especially with noise added to the data, a too sparse data coverage can mean that important features are overlooked or false structures are created. A higher data density improves the resolution significantly at a constant noise level. It is well known that the resolution of surface resistivity investigation decreases strongly with depth, in principle logarithmically. An obvious way to optimise the resolution at depth is to increase the data density, and take measures for improving the data quality during field data acquisition. However, the field data quality aspect is beyond the scope of this paper.

Since only the Wenner array was used, the resolution power of other arrays cannot be compared. It is likely that different electrode arrays offer advantages in resolution in different situations, as well as in terms of logistics, and this deserves further studies.

In real environments, 3D effects will affect the practical resolution of resistivity imaging, and it was not within the scope of this study to assess these effects. There is a risk of creating misleading results when trying to squeeze the most out of a 2D data set from a 3D reality. The most practical way of assessing the relevance of the 2D approach in a field study is to measure a number of parallel lines, and possibly crossing lines as well, to compare how well the results agree. For the future, research on the 3D effects on 2D imaging is called for, as well as development of procedures for 3D inversion of combined 2D data sets.

Acknowledgements

The work behind this paper has received financial support from Swedish Geological Survey (SGU) and Swedish Environmental Protection Agency (AFR/Naturvårdsverket) which is gratefully acknowledged.

References

Barker, R.D., White, C.C., Houston, J.F.T., 1992. Borehole siting in an African accelerated drought relief project. In: Wright, E.P., Burgess, W.G. (Eds.), The Hydrogeology of Crystalline Basement Aquifers in Africa. Geol. Soc. London Spec. Publ. 66, 183–201.

Bernstone, C., Dahlin, T., 1996. Electromagnetic and DC resistivity mapping of waste deposits and industrial sites—experiences from southern Sweden. 58th EAGE Conf., Amsterdam, 3–7 June 1996, M014, 2 pp. (extended abstract).

Carpenter, E.W., 1955. Some notes concerning the Wenner configuration. Geophys. Prospect. 3, 388–402.

Christensen, N.B., Auken, E., 1992. Simultaneous electromagnetic layered model analysis. In: Jacobsen, B.H. (Ed.), Proc. Interdisciplinary Inversion Workshop 1, Aarhus, 1992. Aarhus Univ. GeoSkr. 41, 49–56.

Dahlin, T., 1993. On the automation of 2D resistivity surveying for engineering and environmental applications. Dr. Thesis, ISRN LUTVDG/TVDG–1007–SE, ISBN 91-628-1032-4, Lund Univ., 187 pp.

DeGroot-Hedlin, C., Constable, C., 1990. Occams's inversion to generate smooth two-dimensional models from magnetotelluric data. Geophysics 55, 1613–1624.

Dey, A., Morrison, H.F., 1979. Resistivity modelling for arbitrarily shaped two-dimensional structures. Geophys. Prospect. 27, 106–136.

Loke, M.H., Barker, R.D., 1996. Rapid least-squares inversion of apparent resistivity pseudosections by a quasi-Newton method. Geophys. Prospect. 44 (1), 131–152.

Møller, I., Christensen, N.B., Jacobsen, B.H., 1996. Deconvolution of geophysical multioffset resistivity profile data. In: Jacobsen, B.H., Mosegaard, K., Sibani, P. (Eds.), Inverse Methods. Interdisciplinary Elements of Methodology, Computation and Applications. vol XX of Lect. Notes Earth Sci. XX, pp. 197–204.

Parasnis, D.S., 1986. Principles of applied geophysics, 4th ed. Chapman and Hall, London. 402 pp.

Telford, W.M., Geldart, L.P., Sheriff, R.E., 1990. Applied Geophysics, 2nd ed. Cambridge Univ. Press, 770 pp.

Zhody, A.A.R., 1989. A new method for the automatic interpretation of Schlumberger and Wenner sounding curves. Geophysics 54, 245–253.